Coastal up- and downwelling in the southern Baltic*

OCEANOLOGIA, 47 (4), 2005.
pp. 453–475.

KEYWORDS
Baltic Sea
Upwelling
Downwelling
Hydrodynamic modelling

Marek Kowalewski
Michał Ostrowski

Institute of Oceanography,
University of Gdańsk,
al. Marszałka Piłsudskiego 46, PL–81–378 Gdynia, Poland;

e-mail: ocemk@univ.gda.pl

Received 21 February 2005, revised 23 September 2005, accepted 28 September 2005.

Abstract

A three-dimensional hydrodynamic model was used to determine 12 zones of up- and downwelling in the southern part of the Baltic Sea. On the basis of a seven-year numerical simulation, the annual frequency of up- and downwelling events in various regions was analysed, their vertical velocity evaluated and the probability of their occurrence for different wind directions calculated. Verification of the model results demonstrated their good correspondence with satellite images, on average equal to 92%. The poorest consistency was recorded for upwelling in the Bornholm region (81%). The annual average frequency of strong upwelling (velocities $> 10^{-4}$ m s^{-1}) ranged from c. 5–7% off the eastern coasts of the southern Baltic to $>$ 31% along the north-eastern coast of Bornholm. Along the Polish coast (excepting the Vistula Spit) downwelling was recorded more frequently than upwelling. The frequency of strong vertical currents was highest in the area to the north of the Hel Peninsula, where high percentages of strong upwelling (27.1%) and downwelling (37.1%) were recorded.

* This research was supported by the State Committee for Scientific Research, Poland (grant No 6 P04G 061 17). Editing assistance of the article was provided by BALTDER (EVK3-CT-2002-80005), funded by the European Commission under the 5th Framework Programme.

1. Introduction

Upwelling is a vertical current, usually occurring near the coast, which leads to an upward movement of water from deeper layers to the sea surface. Owing to the very small velocities involved – c. 10^{-4} m s^{-1} – direct measurement of vertical flows related to upwelling is extremely difficult. In practice, however, these events can be detected indirectly as a result of their effects on temperature and salinity stratification in the sea.

The formation of coastal upwelling is related to the Earth's rotation. According to Ekman's theory, the Coriolis force causes currents to be deflected to the right in the northern hemisphere, and to the left in the southern hemisphere. When a local, longshore wind is blowing, Ekman transport causes surface water to move on- or offshore. In the first case, a flow towards the coast will cause local sinking of surface waters (downwelling), in the second a flow of water away from the coast will be compensated by a rise of deeper water (upwelling). This implies that in the northern hemisphere an upwelling event can occur when a current flows along a coast lying to the left of the velocity vector (Bowden 1983).

Coastal upwelling in the Baltic Sea is rather poorly understood. This is due to methodological difficulties, since such events are irregular and not at all widespread. The first papers describing local, accidental observations of upwelling were published in the 1970s. Walin (1972a) recorded upwelling in Hanö Bay, and associated its formation with an atmospheric front. He also observed disturbances in the temperature field, drifting along the coast in a similar manner to Kelvin waves (Walin 1972b). Svansson (1975) registered upwelling in the western part of Hanö Bay in both summer and winter. Schaffer (1979) observed such events off the west coast of Gotland.

In the early eighties, satellite remote sensing methods came into use, making it possible to register water surface temperatures over large areas, and this led to substantial progress in upwelling research. Analysing an image from an AVHRR radiometer installed on NOAA satellites, Horstman (1983, 1986) detected upwelling induced by easterly winds off the southern shores of the Baltic Sea. Gidhagen (1984, 1987) analysed upwelling off the Swedish coast: with the aid of *in situ* measurements and satellite images (in the summer), he concluded that upwelling occurs most often in the presence of strong north-westerly winds and that the frequency of their occurrence in some regions is $> 30\%$. On the basis of hourly temperature measurements, Zakharchenko & Kostyukov (1987) described falls in water temperature in the southern part of the Gulf of Riga from 6 to 128 hours in duration, and associated this with the rise of deeper waters. On the basis of satellite image analysis Bychkova & Viktorov (1987) identified 14 upwelling zones in the Baltic Sea. They presented basic specifications, such as their extent, typical wind conditions, and worked out temperature gradients for each zone. Bychkova et al. (1988) presented a more detailed list for the entire Baltic Sea of 22 upwelling zones related to atmospheric circulation. On the basis of the water temperature data measured on lightships and at coastal stations, they specified the duration and frequency of upwelling. The dynamics of upwelling to the north-west of Rügen was examined by Fennel & Sturm (1992) and by Lass et al. (1994) using satellite images, *in situ* measurements and a hydrodynamic model. Research on upwelling along the Hanko Peninsula, on the border of the Gulf of Finland and the Baltic Sea, was carried out by Haapala (1994). These events were detected as an abrupt increase in salinity (by around 1 PSU) at a depth of 35 m. Urbański (1995) analysed upwelling in relation to the velocity and direction of the wind along the Polish coast. In contrast to the results obtained by Gidhagen (1987), he discovered that upwelling occurs mainly when winds were weak, < 4 m s^{-1}, and with a frequency of 26%. Similar results were obtained by Krężel (1997b), who studied upwelling in the southern Baltic.

Nevertheless, such research into coastal upwelling in the Baltic Sea as has been carried out so far is still in its infancy. Most of the information at our disposal has come from satellite observations. Even so, remote sensing methods have numerous limitations preventing a thorough understanding of the factors governing upwelling in the Baltic. Upwelling can only be registered on a satellite image when the sky is clear, and when the temperature of surface waters differs significantly from that of deeper waters. Because of these limitations, remote sensing analysis of upwelling is only done in the Baltic in the warmer half of the year. Few reliable data are therefore available on the frequency of upwelling or calculations of vertical flow velocities in the regions where it occurs. To fill this gap is one of the aims of the present study. As yet there is very little information about coastal downwelling in the Baltic Sea. Remote sensing methods cannot be used to investigate this particular phenomenon, and since direct measurement of vertical flow velocities is very difficult, the only practical way of examining such events is to model them mathematically.

Because of the difficulties involved in investigating upwelling by remote sensing techniques, numerical hydrodynamic models are increasingly gaining favour (Kowalewski 1998, Jankowski 2002, Lehmann et al. 2002, Myrberg & Andreyev 2003). To estimate the frequency of upwelling events, a three-dimensional hydrodynamic numerical model has been used (Kowalewski 1997). With such a model, vertical velocities can be calculated for a given thermohaline stratification and set of wind conditions; hence, the frequency of these events and the wind conditions related to their formation can be analysed.

2. Hydrodynamic model

The research methodology of up- and downwelling in the Baltic is founded upon numerical experiments that use a three-dimensional hydrodynamic model of this sea based on the Princeton Ocean Model (POM), which has been used in research into coastal upwelling (Blumberg & Mellor 1987). Adapting the POM to Baltic conditions has required a few changes in the numerical calculation scheme. Details of the application of the hydrodynamic model to Baltic Sea can be found in Kowalewski (1997).

Coastal up- and downwelling events are small, so any model of them must possess a high resolution. The results of simple upwelling models show that in the case of a stratified sea (Bowden 1983), such events occur in coastal zones of a width equal to Rossby's barocline radius. In the Baltic Sea, the deformation radius in the case of thermal stratification is a few kilometres. This means that in order to model coastal upwelling reliably, a numerical grid with a small grid size (i.e. smaller than Rossby's deformation radius) should be used. But decreasing the grid spacing requires the time step to be limited, and this in turn significantly lengthens the computer calculation time. Therefore, in our work, a compromise solution based on local grid condensation had to be applied – sub-areas were separated by smaller time and space steps. A numerical grid with a grid spacing of c. 5 NM was applied to the whole Baltic Sea, and a smaller grid with a 1 NM spacing was used for the southern Baltic (Fig. 1). Vertically, both areas were divided into 18 layers. The same number of layers at every sea point, irrespective of depth, was obtained by sigma-transformation. The individual layers were of different thickness: 8.3% of the depth in the

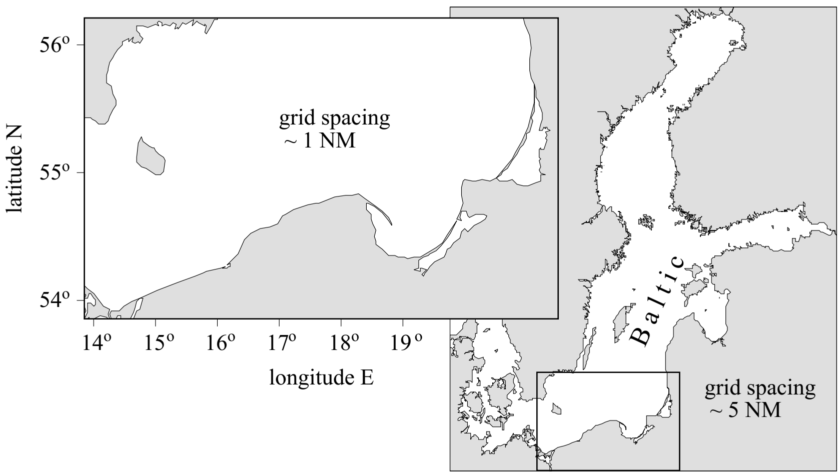

Fig. 1. The area covered by the model

middle of the profile, 2.0% at the bottom and 0.5% at the sea surface. By using thinner layers, a better mapping of the surface and bottom layers was obtained. On the open border between the Kattegat and the Skagerrak a vertically averaged radiation boundary condition for the flows was applied.

3. Upwelling and downwelling regions

Simplified calculations were performed to determine the zones of up- and downwelling. A unified, vertical temperature profile characteristic of August (Lenz 1971) was applied to the whole Baltic Sea (Fig. 2). The initial salinity field was obtained by interpolating the August climate data (ICES 1969–1980, Bock 1971). These simulations were carried out on the assumption of zero heat exchange through the sea surface and stable winds of 10 m s^{-1} from the 8 basic directions. The components of the surface wind stress vector, τ_{ox} and τ_{oy}, were computed according to the formulas

$$\tau_{0x} = C_D \rho_{atm} \sqrt{U_{10}^2 + V_{10}^2}\, U_{10},$$

$$\tau_{0y} = C_D \rho_{atm} \sqrt{U_{10}^2 + V_{10}^2}\, V_{10},$$

where

ρ_{atm} – density of the atmosphere,

C_D – drag coefficient (0.0026),

U_{10}, V_{10} – wind velocity components at 10 m above sea level.

A 24-hour simulation yielded sea surface temperature distributions for the southern Baltic (Fig. 3), where regions of upwelling were clearly visible as zones of significantly lower temperature. According to Ekman's theory, upwelling zones may be present in various regions depending on the wind direction. In the area under scrutiny here, the most upwelling zones were detected with E and SE winds; when they are blowing from these directions, upwelling occurs along almost the entire southern coast of the Baltic. The exception is the Pomeranian Bay: upwelling does not occur there because its waters are too shallow. In the eastern Baltic the zone of upwelling lies farther away from the coast. An upwelling map (showing all 12 regions under study here) was drawn by calculating the deviations of minimum water temperatures for all eight wind directions. The method of upwelling determination applied here was analogous to remote sensing methods. Nevertheless, the regions determined by this method were rather large, since the upwelled cold water undergoes advection and mixing.

In order to find upwelling zones in a dynamic sense, i.e. zones of rising current, vertical velocities for the same eight model simulations were calculated (Fig. 4). Vertical velocities at 20 m depth were analysed, since

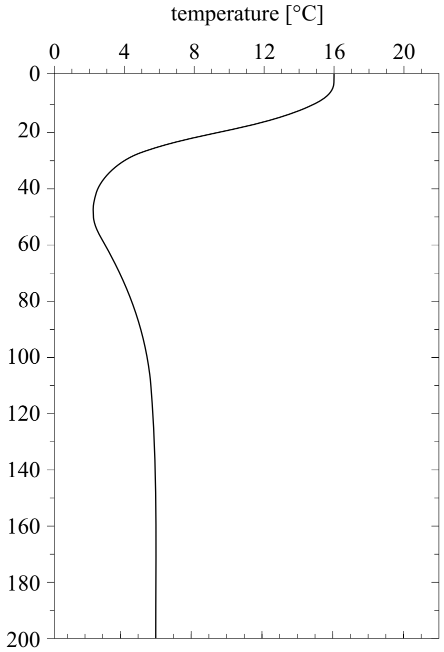

Fig. 2. The water temperature profile, assumed as an initial condition in the model

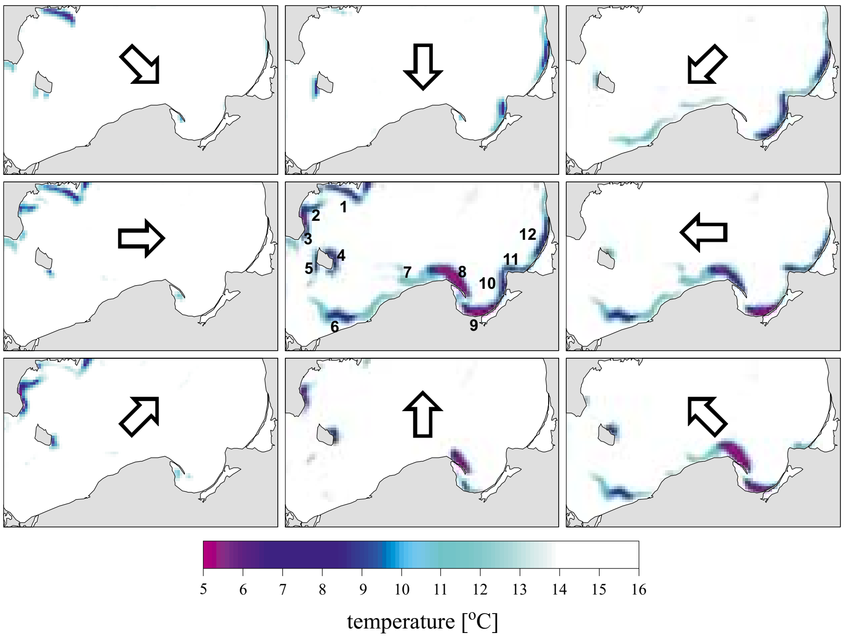

Fig. 3. Distributions of surface water temperatures in the southern Baltic Sea, calculated after 24 hours of wind activity (velocity 10 m s^{-1}) from the 8 basic directions, and the minimum temperatures determined on their basis (middle image). The numbers mark the regions of upwelling

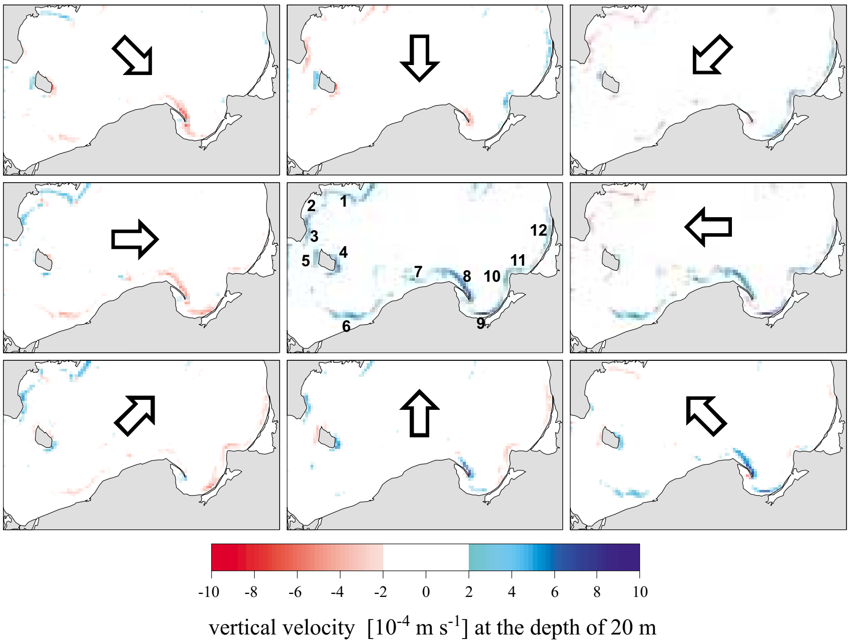

Fig. 4. Vertical velocity distributions in the southern Baltic at 20 m depth, calculated after 24 hours of wind activity (velocity 10 m s^{-1}) from the 8 basic directions, and the maximum vertical velocities determined on their basis (middle image). The numbers mark the regions of upwelling

the vertical flows were the strongest at this depth. Fig. 4 presents vertical flows of velocity $> 2 \times 10^{-4}$ m s^{-1}. Evidently, up- and downwelling events occur in almost the same locations, but with winds from opposite directions, and this provides the opportunity of analysing these phenomena in the same areas.

Up- and downwelling zones were determined in such a way that the regions with the highest vertical velocities could be identified. They were determined as regions where, for at least 2 adjacent wind sectors, velocities $> 2 \times 10^{-4}$ m s^{-1} were recorded. These regions are therefore zones of strong vertical currents. It should be noted that the simulation period (24 hours) and depth (20 m) set-up was arbitrary. However, when the areas were determined under slightly different assumptions, they differed only in extent, but not location.

4. Verification of model results on the basis of satellite data

121 AVHRR thermal images from NOAA satellites registered in the summer half-year were used to verify the consistency of the place and time of upwelling formation generated by the model. For this period it is

relatively easy to identify areas of upwelling from an analysis of the spatial distributions of sea surface temperatures (SST). The satellite images were taken during April–October: five in 1996, two in 1998, 44 in 2000, and 70 in 2001. Only the cloud-free areas on each image were subjected to analysis.

In order to verify and calculate the upwelling/downwelling frequency, a long-term simulation based on a hydrodynamic model with real meteorological conditions (wind field, air temperature, atmospheric pressure and vapour pressure) was carried out. Two periods were modelled: 1994–96 and 1998–2001. For the first period, 6-hour averaged meteorological data from the ECMWF (European Centre for Medium-Range Weather Forecasts) weather model were used. The data for the second were obtained from the UMPL (Unified Model for Poland) mesoscale weather model and used at 3 hour intervals. The solar energy inflow (Krężel 1997a), heat exchange through the sea surface (Jędrasik 1997) and inflows from the 125 largest rivers (Cyberski 1997) were also taken into account. In both periods climatic salinity and temperature distributions for January (ICES 1969–1980, Bock 1971, Lenz 1971) were applied as initial fields.

To verify the consistency of the methods, the distributions of sea surface water temperatures as determined by satellite images and generated by the model were compared (Fig. 5). Determining upwelling on a satellite image amounted to finding an area of water whose temperature was lower than that of the surroundings. If a precise classification could not be made, the situation was excluded from the verification process. If the model results were uncertain, the vertical flow field was also analysed.

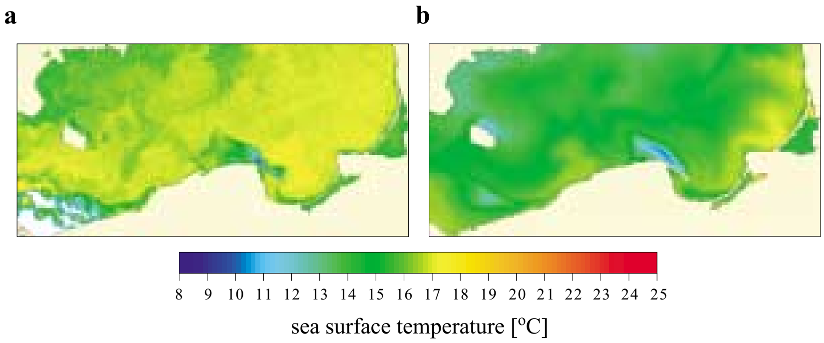

Fig. 5. A comparison of upwelling regions determined from an analysis of the surface temperature distributions for 17th September 2000 on the satellite image (NOAA 14) (a) and generated by the model (b); the colour scale is identical for both images

Fig. 5 compares sea surface temperature observations from satellite images and those calculated by the model for a particular day (17.09.2000).

In both cases, upwelling in the region of the Hel Peninsula (region 8) and off the north-east coast of Bornholm (region 4) was visible. Cool water was also present close to Kołobrzeg (region 6) on a partially cloud-covered satellite image, as well as along the Vistula Spit (region 9) – in both of these zones, cool waters were identified as upwelling waters. The upwelling in region 6 was much clearer on the satellite image than in the model result. The model also generated upwelling in regions 1–3, off the southern coasts of Sweden. However, it was impossible to tell from the satellite images of this region if the cooling of the water had indeed been caused by upwelling. The surface area of cool water regions on the image was actually rather smaller than in the model results: this was most evident off the Bornholm coast, where the model generated an upwelling event much larger than that recorded by the satellite data.

For each region, a set of cloud-free AVHRR images was chosen from the 121 available for analysis. From 46 (region 3) to 77 (region 10) situations were analysed. Upwelling was most often evident in both image and model results in regions 7 and 8, least often in region 5 (Table 1). Situations where upwelling or its absence were observed in both image and model results were classified as consistent. Consistency was greatest (> 95%) in regions 2, 5, 7, 9 and 12. Consistency was lowest (80.6%) in region 4; here, the model generated upwelling distinctly more often than was recorded on the satellite images. In general, it can be stated that the model estimated the time and area of upwelling relatively well (92% consistency). However, a tendency for

Table 1. A comparison of upwelling events recorded on satellite images with those generated by the model

Region	Number of cases analysed	Upwelling		Consistent conditions	
		Satellite images	Model	Number	[%]
1	57	13	21	47	82.5
2	48	12	14	46	95.8
3	46	9	12	43	93.5
4	62	10	20	50	80.6
5	67	4	5	64	95.5
6	56	21	18	51	91.1
7	68	24	26	66	97.1
8	73	30	35	63	86.3
9	68	14	17	65	95.6
10	77	12	13	72	93.5
11	76	14	11	71	93.4
12	73	21	18	70	95.9
Total	771	184	210	708	91.8

upwelling to be overestimated is noticeable in the model results as compared to the satellite observations, with the exception of regions 6 and 11. Here upwelling was recorded on the images more often than in the model results.

5. Frequency of upwelling and downwelling

During the long-term simulation, the average daily vertical velocities at 20 m depth were calculated for each day (2556 days in total over two periods: 1994–96 and 1998–2001). This provided the opportunity of calculating the frequency of up- and downwelling separately in each region (Table 2). Because in practice the vertical velocity at a given locality is never exactly equal to zero, any situation can be classified as up- or downwelling: however, these terms imply relatively strong flows. It was therefore decided to divide up- and downwelling events into 'strong' and 'weak' classes, with respective velocities of $> 10^{-4}$ m s^{-1} and $< 10^{-4}$ m s^{-1}. Vertical velocities in the sea are always distributed continuously, hence such a division of up- and downwelling into two classes is arbitrary – it requires a boundary velocity to be determined above which the phenomenon is regarded as strong. For the purposes of comparing the frequency of up- and downwelling with data from earlier studies, which were based mainly on satellite image analysis, strong up- and downwelling events correspond to those data obtained by remote sensing methods. Assuming the thickness of the mixed layer to be 10-20 m in the warm half-year, upwelling of e.g. 10^{-5} m s^{-1} would be recorded at the sea surface after 12–23 days. It is highly improbable that in the Baltic region the wind will blow from the same direction for

Table 2. Upwelling and downwelling frequency (percentage) in particular regions of the southern Baltic

Region	Upwelling			Downwelling		
	$< 10^{-4}$ m s^{-1}	$> 10^{-4}$ m s^{-1}	Total	$< 10^{-4}$ m s^{-1}	$> 10^{-4}$ m s^{-1}	Total
1	34.0	17.6	51.6	37.8	10.6	48.4
2	30.1	23.5	53.6	32.0	14.4	46.4
3	36.1	16.4	52.5	35.0	12.5	47.5
4	41.7	31.1	72.8	18.1	9.1	27.2
5	32.4	18.1	50.5	34.2	15.3	49.5
6	37.2	11.8	48.9	35.4	15.6	51.1
7	35.3	6.3	41.6	45.3	13.1	58.4
8	15.5	27.1	42.6	20.3	37.1	57.4
9	35.7	18.8	54.5	30.3	15.2	45.5
10	37.1	5.8	42.9	46.4	10.7	57.1
11	39.4	7.3	46.7	45.3	8.0	53.3
12	40.2	4.6	44.8	45.3	9.9	55.2

such a long period; therefore, a minimum vertical velocity of 10^{-4} m s^{-1} was chosen at which the wind inducing upwelling would have to persist for 28–56 hours. A velocity of 10^{-4} m s^{-1} is equal to a water rise of 8.64 m per day. Under Baltic Sea conditions, this value can be considered the minimum velocity permitting upwelling to be detected on the sea surface, and therefore recorded on satellite images.

The results indicate a large differentiation of the phenomena under discussion. Upwelling events, strong ones in particular, were dominant along the Swedish coast (regions 1, 2, 3) and around Bornholm (regions 4, 5) (Fig. 6). The rest of the region was dominated by downwelling, except for the waters along the Vistula Spit in the Gulf of Gdańsk (region 9), where upwelling occurred more often. Most of the strong upwelling events (31%) were registered in region 4 (along the north-east coast of Bornholm), and most of the weak ones were also recorded in this region (42%), which makes a total percentage of these events of 73%. Most of the strong downwelling events occurred (c. 37%) in region 8, off the north coast of the Hel Peninsula; however, most of all the downwelling events (strong and weak) were recorded in region 7.

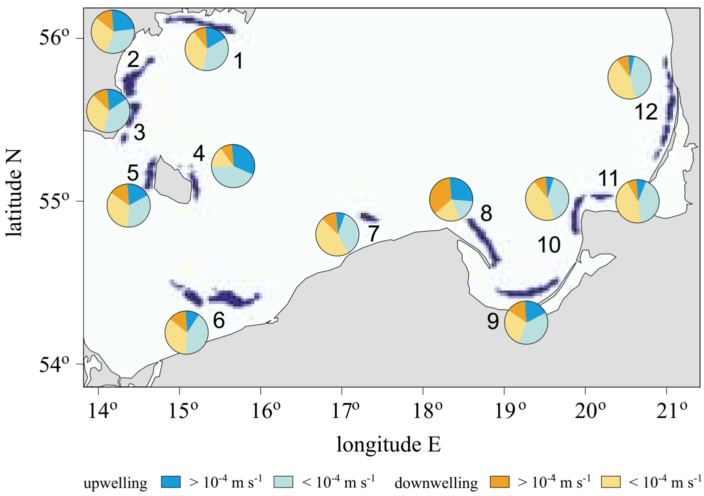

Fig. 6. Upwelling and downwelling frequency in particular regions

It is also worth pointing out that in some regions the percentage of strong vertical currents ($> 10^{-4}$ m s^{-1}) was high, while in others it was small. Strong vertical flows occurred most often in region 8, where the overall percentage of strong up- and downwelling events was 63%, and least often in region 11 (c. 15%).

The results of the analysis for the 12 regions are presented in Fig. 7.

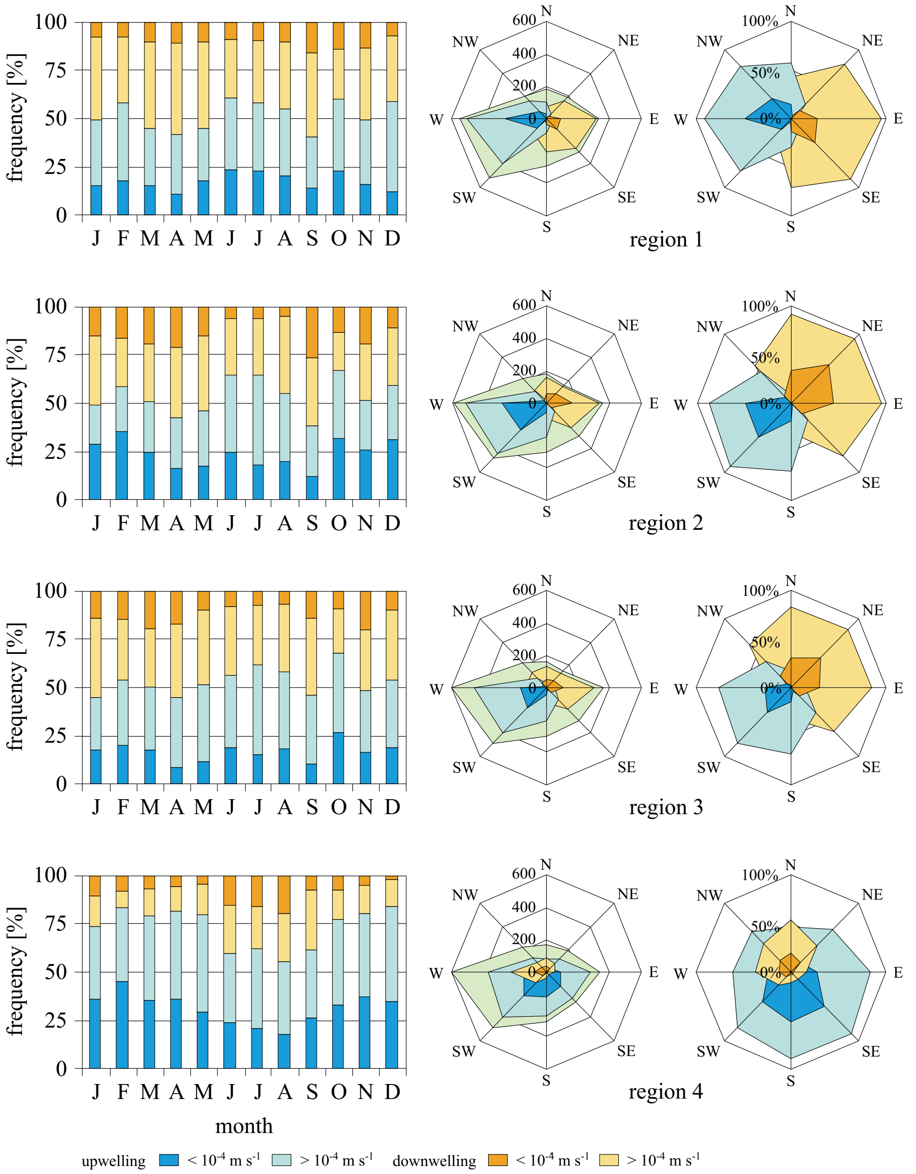

Fig. 7. Left: the frequency (%) of up- and downwelling events in the various southern Baltic regions during different months. Middle: the occurrence of up- and downwelling events and winds from a given sector, according to wind direction. Right: the probability (%) of up- and downwelling events, depending on wind direction

The frequency of up- and downwelling in the given months was calculated, and the probability of up- or downwelling occurring depending on wind direction was analysed. The dominant wind direction in a particular region

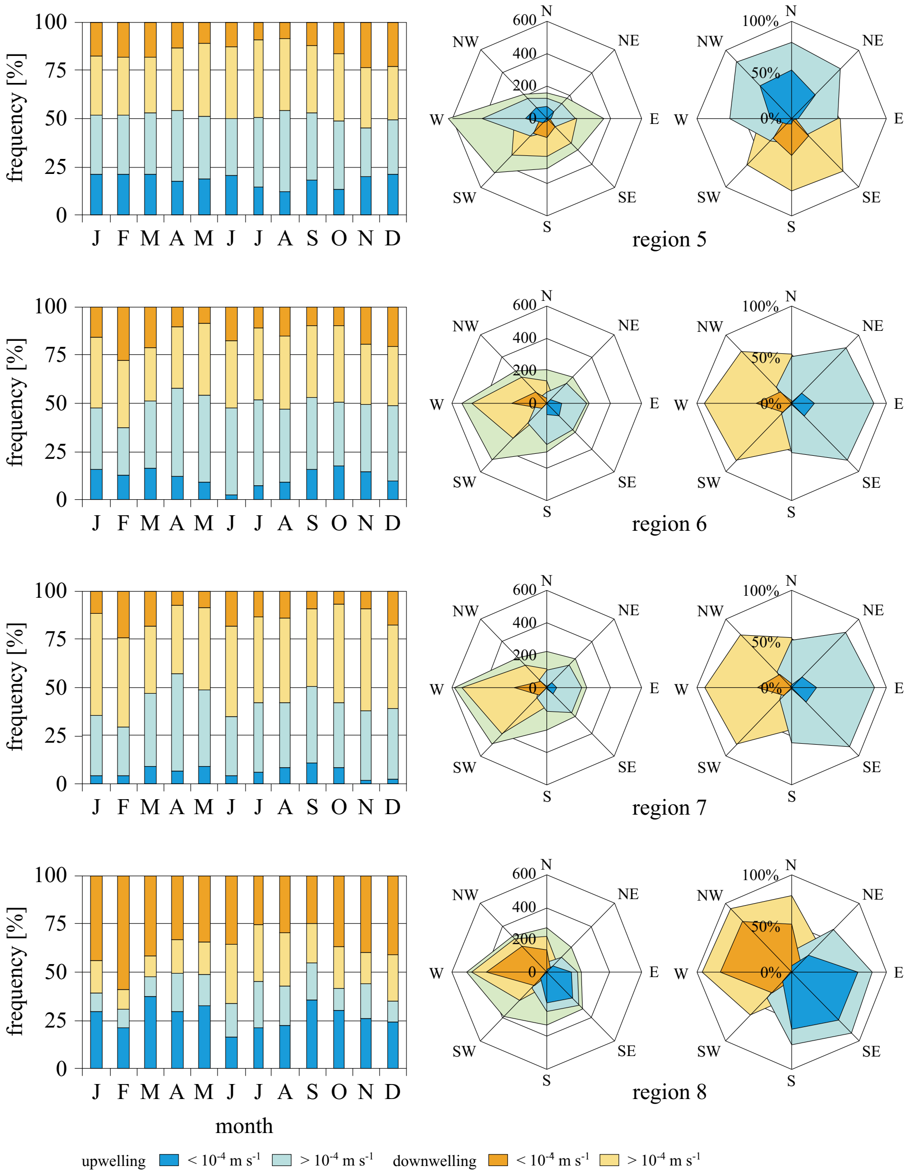

Fig. 7. (*continued*)

was determined for each of the 2556 days of the simulation. By dividing the number of days when up- or downwelling occurred for a chosen wind direction by the total number of days with the wind blowing from a given sector, the probability of an up- or downwelling event for the chosen wind direction was obtained.

In Hanö Bay (regions 1, 2 and 3) upwelling is the rule mainly in summer

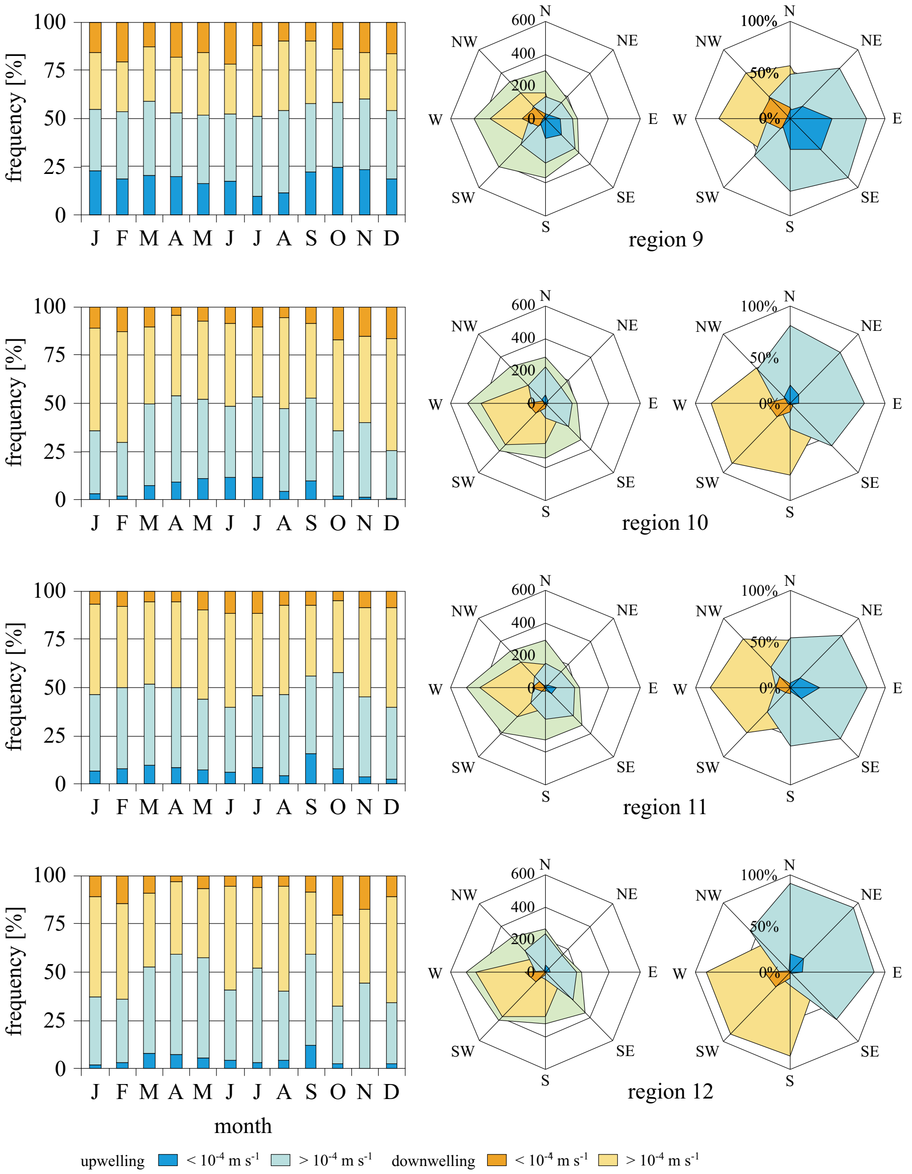

Fig. 7. (*continued*)

and winter, downwelling in autumn and spring. The prevalence of westerly and south-westerly winds, which are responsible for the high probability of upwelling events, means that they occur throughout the year. In regions 1 and 2 the majority of downwelling events take place in September, most upwelling events in June. In region 3 downwelling occurs most often in November, upwelling in October.

The areas adjacent to Bornholm are significantly different. In region 4 upwelling was clearly dominant, with a mean annual percentage in excess of 73%, and in autumn, winter and spring it often exceeded 80%. However, upwelling events were also dominant in summer, when they were least numerous (c. 60%). The most upwelling events were observed in February and the fewest in August. This situation is difficult to explain, since the prevailing winds in this region are westerlies, which should lead to downwelling. However, for westerly winds the probability of upwelling is higher than that of downwelling. This implies the existence of an additional factor generating upwelling. The probability of downwelling was greater here only for northerly winds, which are very rare in this region. On the other side of Bornholm, in region 5, up- and downwelling occurred with a similar frequency: most upwelling events occurred in January, downwelling in February. The greatest probability of upwelling was recorded with winds from the north and north-west, while downwelling events were most likely with winds from the south.

Located along the Polish coastline, regions 6, 7 and 8 have many features in common. In all these zones downwelling was dominant, which is a consequence of the prevailing westerly winds. Most upwelling events occur here in April, May and September, with downwelling taking place in February. Of these three zones, region 8 was the most distinctive with the highest percentage of days with strong vertical currents ($> 10^{-4}$ m s^{-1}) in the southern Baltic: for example, in February strong downwelling occurred on c. 60% of days and intensive upwelling on 20% of days. In regions 6 and 8 the probability of upwelling was highest when winds were from the southerly to north-easterly sectors, and in region 7 when they were from the south-easterly to north-easterly sectors.

Located along the Vistula Spit in the Gulf of Gdańsk, region 9 is characterised by the dominance of upwelling over downwelling: this is the only region on the south coast of the Baltic where this happens. The frequency of upwelling was higher in every month, most of all in autumn, and least of all in July. The dominance of upwelling is surprising considering the fact that the prevailing winds are westerlies: they should cause downwelling. However, it turns out that in this region there is a greater probability of upwelling than downwelling.

The three remaining regions (10, 11, 12) were located in the eastern Baltic and were characterised by a small percentage of strong vertical currents, from 14% to 16% annually, downwelling being slightly the more dominant. In region 10 (eastern Gulf of Gdańsk) most upwelling events occurred in spring and summer, while in regions 11 and 12 they took place most often in September. Downwelling was dominant in autumn and winter in regions 10 and 12, but from May to August in region 11. In these regions, as in the whole of the southern Baltic, the prevailing winds, causing downwelling, are from the west. The percentage of easterly and north-easterly winds, which cause upwelling, is very small. The probability distribution of the occurrence of vertical currents is consistent with the direction of the coastline.

6. Vertical velocities in the upwelling regions

The relationships between vertical velocity and wind velocity in the particular regions are shown in Fig. 8. The vector component of the wind velocity parallel to the coastline was used in the calculations because it is the one responsible for coastal up- and downwelling. The linear regression and squared coefficient of correlation equations are shown in the same figure. With the linear regression equation the vertical velocity in a particular region can be estimated from a known wind velocity. It is therefore possible simply to assess up- or downwelling occurrences on the basis of weather reports.

The highest correlation coefficient of 0.91 was registered in region 2, the lowest – 0.53 – in region 4. This means that in the first case, the change in wind velocity (the component tangential to the coastline) explains 82% of the vertical velocity changes, but in the second case only 28%. It may therefore be assumed that in region 4 some factors other than wind velocity are responsible for the dominance of upwelling. This view is also endorsed by the large value of the bias in the regression formula, which means that even with no wind, upwelling occurs with a velocity of 4.1×10^{-5} m s^{-1}. The slope of the regression line shows how easily the longshore wind brings about the vertical current. The slope coefficient of the regression for most of the cases ranged from 0.1 to 0.25. The Hel Peninsula area was an exception (region 8): there the coefficient was 0.42, which means that both up- and downwelling form here very easily, that is to say, even when winds are relatively weak.

The vertical velocities (Table 3) calculated as annual averages and over a seven-year period confirm the results obtained from the analysis of up- and downwelling frequency. The highest positive value was obtained for region 4 (north-eastern Bornholm). The average value of 5.5×10^{-5} m s^{-1} indicates that upwelling there is permanent, with water moving up towards the surface by an average of 5 m per day. A second zone of upwelling dominance is located off the western coast of Hanö Bay (region 2). The dominance of downwelling was most evident in region 8, along the Hel Peninsula, where the average velocity was 2.6×10^{-5} m s^{-1} (2.2 m d^{-1}).

Although minor year-to-year differences are noticeable (Fig. 9), in general the average vertical velocity distributions are largely similar.

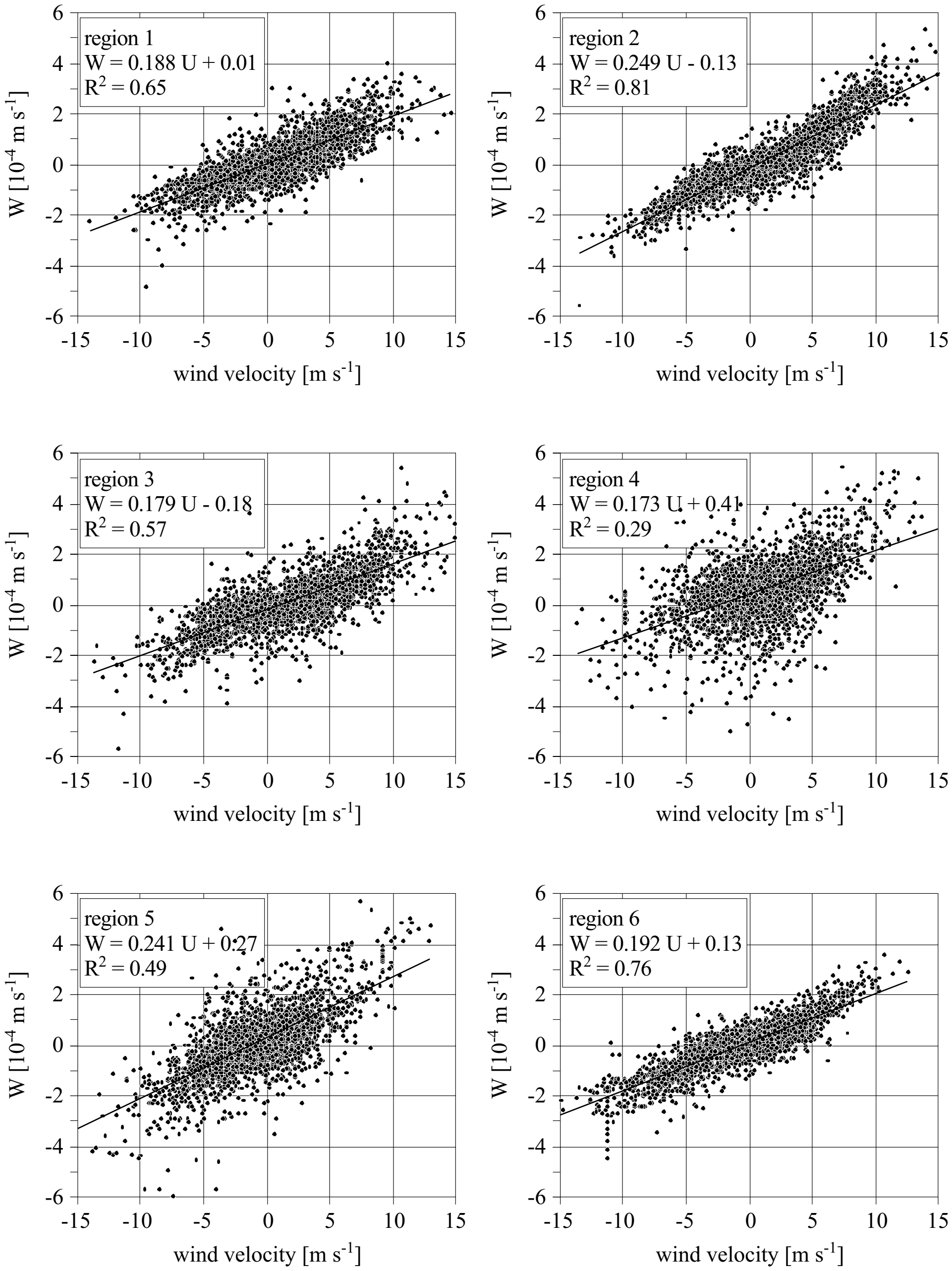

Fig. 8. The relationship between vertical water velocity (W) and wind velocity tangential to the coastline in particular regions of upwelling occurrence

Region 8 takes on a particular significance owing to the large downwelling area in the vicinity of Hel. Considering the high average velocities, it is

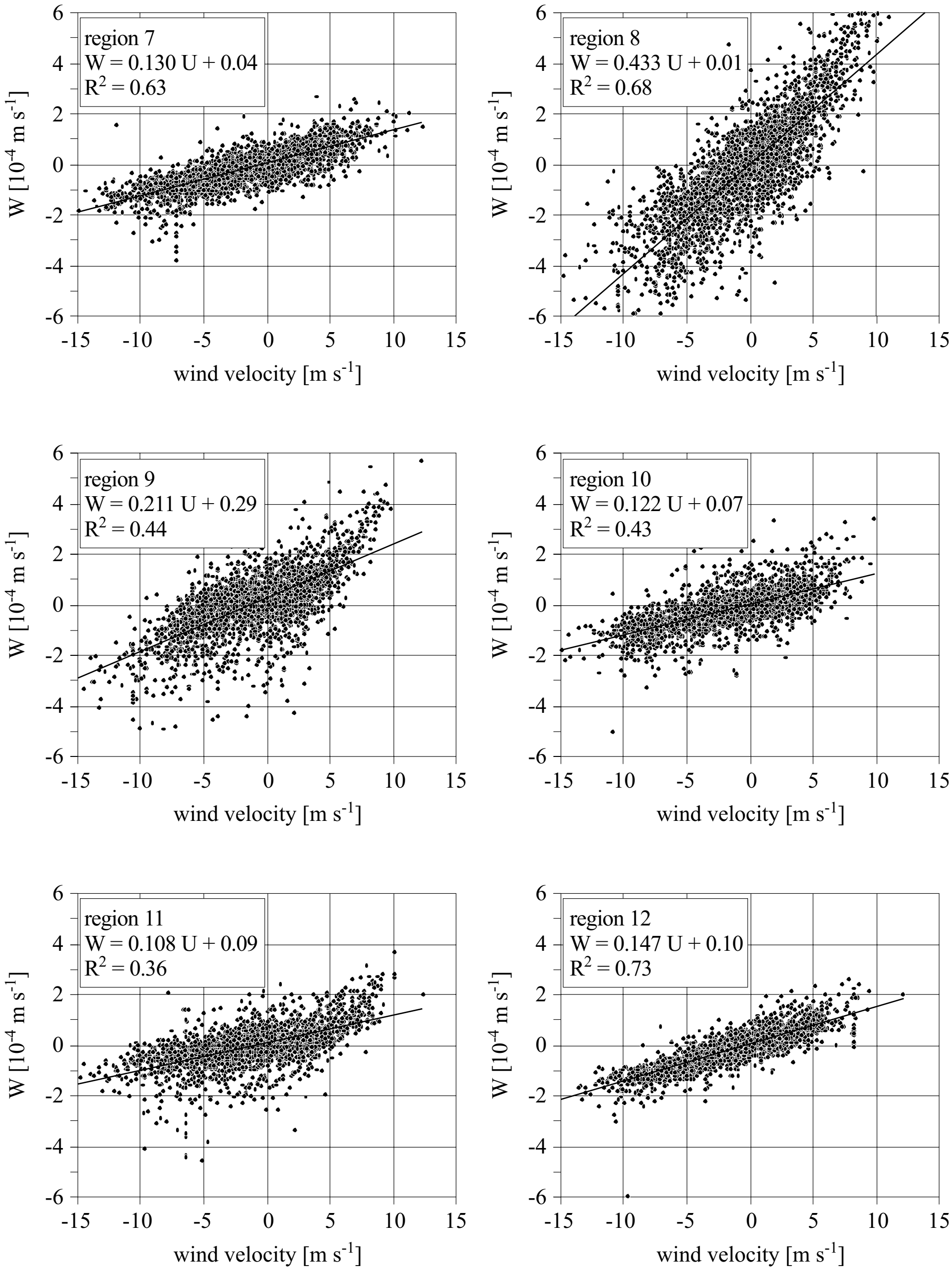

Fig. 8. (*continued*)

a water sink of some significance. Even though it is generally a downwelling zone, the area around the tip of the Hel Peninsula is dominated by upwelling. Such adjacency of downwelling and upwelling zones is also characteristic

Table 3. Average vertical velocity (10^{-4} m s^{-1}) at 20 m depth calculated in particular regions of the southern Baltic during 1994–96 and 1998–2001

Year	Region											
	1	2	3	4	5	6	7	8	9	10	11	12
1994	0.21	0.33	0.06	0.18	0.16	–0.13	–0.24	–0.42	–0.09	–0.11	–0.10	–0.14
1995	0.20	0.32	0.10	0.53	0.00	–0.08	–0.20	–0.41	0.06	–0.12	–0.08	–0.13
1996	0.10	–0.05	–0.05	0.48	0.06	0.05	–0.08	–0.06	0.13	–0.02	0.07	0.08
1998	0.13	0.30	0.10	0.54	0.23	–0.15	–0.22	–0.47	0.21	–0.14	–0.01	–0.17
1999	0.04	0.27	0.17	0.77	–0.10	–0.04	–0.15	–0.21	0.20	–0.14	–0.05	–0.19
2000	0.04	0.37	0.24	0.78	–0.08	0.01	–0.11	0.01	0.15	–0.15	0.00	–0.14
2001	0.10	0.12	0.08	0.54	0.26	–0.09	–0.13	–0.36	–0.01	–0.14	–0.16	–0.10
Total	0.12	0.24	0.10	0.55	0.08	–0.06	–0.16	–0.27	0.09	–0.12	–0.05	–0.11

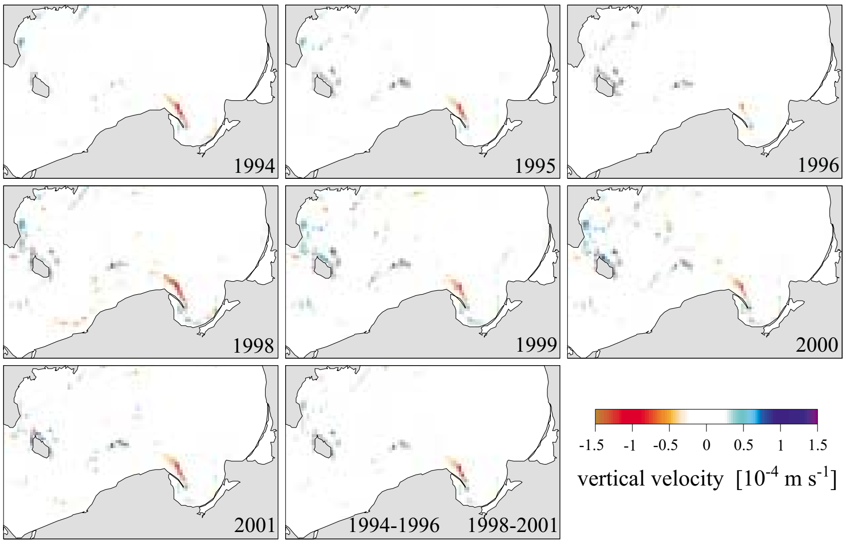

Fig. 9. The distribution of the average vertical velocity at 20 m depth calculated on the basis of the model simulation for the periods 1994–96 and 1998–2001

of the other regions. Apart from the zones of strong vertical currents located in the coastal area (Fig. 9), there are also down- and upwelling zones located further away from the coast, e.g. in the Słupsk Furrow or Bornholm Deep. However, as these are not related to coastal up- and downwelling phenomena, they were not analysed.

7. Discussion and conclusion

By applying the three-dimensional hydrodynamic model, 12 regions of coastal up- and downwelling could be identified in the southern Baltic Sea.

Ten of these regions have already been described in the literature (Bychkova & Viktorov 1987, Bychkova et al. 1988, Urbański 1995, Krężel 1997b); the other two regions (4 and 5) are located around Bornholm. These zones are very small, located close to the coast, and picking them out on satellite images is quite tricky. Nevertheless, upwelling was identified in these regions during the satellite image analysis performed for the purposes of verifying the model. In 10 out of 62 cases analysed in region 4, cool water most probably related to upwelling was recorded. Fig. 5a is an example of an upwelling event in region 4. Only four upwelling events of the 67 examined in region 5 were picked up on the satellite image.

Verification of the model displayed a high consistency between the upwelling events generated by the model simulations and those seen on satellite images. On average, 92% of the cases were consistent – only in region 4 did larger inconsistencies appear (19%).

So far, attempts at estimating the frequency of upwelling events have been based mainly on the analysis of surface water temperature changes measured at coastal stations and on lightships (Gidhagen 1987, Bychkova et al. 1988) or on satellite image analysis (Krężel 1997b). Both approaches require the presence of thermal stratification; in practice, then, they are restricted to the warm half of the year. By additionally including salinity, sea level, air temperature, and wind direction and velocity, Urbański (1995) was able to estimate the average annual frequency of upwelling along the Polish coast at 26%. All earlier attempts had been based on the analysis of the effects of upwelling, mainly the drop in surface water temperature. The application of a numerical model has made research into the frequency of upwelling possible in accordance with its original definition as a rising current. However, the question arises whether even the slowest vertical current can be classified as up- or downwelling. If this assumption were made, then, remembering that the probability of the vertical velocity at any point at the sea being exactly zero is very small, this would mean that up- or downwelling is always taking place. Vertical currents were therefore divided into strong and weak ones. Upwelling frequencies calculated on the basis of temperature measurements should be compared with strong upwelling events ($> 10^{-4}$ m s^{-1}), since only rising currents of such a strength are capable of lifting water from deeper layers up to the surface.

The methodological differences in the research are such that good consistency should not be expected between earlier research and the results of this study. One of the reasons is that there may be a few days' delay between the occurrence of upwelling (rising current) and the subsequent drop in surface water temperature. Cool water raised to the surface as a result of upwelling can remain there for many days even after the actual upwelling has ceased in a dynamic sense.

This research also showed that upwelling was dominant along the Swedish coast, where the frequency ranged from 16.4% to 23.5%. These results are generally consistent with the values given by Gidhagen (1987) for the Karlshamn station (region 1 – north shore of Hanö Bay) in July, August and September: 18%, 23% and 20%, respectively. The strong upwelling frequencies calculated for the same months based on the model simulations for region 1 were 23%, 21% and 14%, respectively. In August the upwelling frequency for the Sandhammaren station (region 3) was estimated by Gidhagen (1987) at 11%, while the model research produced a value of 18%.

The model calculations showed that upwelling in the southern Baltic occurred most frequently in region 4 (north-eastern coast of Bornholm); this is not mentioned anywhere in the literature. The upwelling frequency in this region was 72.8%, including 31.1% of strong upwelling events, which means that it is an area of almost permanent upwelling. Unfortunately, the reliability of the model results for this region is not perfect, since validation yielded only 80.6% consistency.

The regions located along the Polish coast were characterised mainly by downwelling, which is related to the prevalence of westerly winds in the area. The strong upwelling frequency of 11.8%, calculated for region 6, is significantly different from the value of 26% given by Urbański (1995). Region 8, to the north of the Hel Peninsula, is a region of very pronounced vertical currents. But even though the percentage of strong upwelling there is high (27.1%), downwelling is still dominant (37.1%). Region 9 (along the Vistula Spit) was the only one along the southern Baltic coast where the dominance of upwelling over downwelling was recorded, even though westerly winds, which should cause downwelling, are dominant here. This means that there must clearly be some other factors, e.g. related to coastline formation, which induce upwelling rather than downwelling.

References

Blumberg A. F., Mellor G. L., 1987, *A description of the three-dimensional coastal ocean circulation model*, pp. 1–16, [in:] *Three-dimensional Coastal Ocean Models*, N. S. Heaps (ed.), Am. Geophys. Union, Washington, 208 pp.

Bock K.-H., 1971, *Monatskarten des Salzgehaltes der Ostsee, dargestellt für verschiedene Tiefenhorizonte*, Dt. Hydrogr. Z., 12, 148 pp.

Bowden K. F., 1983, *Physical oceanography of coastal water*, Ellis Horwood Ltd., Chichester, 302 pp.

Bychkova I. A., Viktorov S. V., 1987, *Use of satellite data for identification and classification of upwelling in the Baltic Sea*, Oceanology, 27 (2), 158–162.

Bychkova I. A., Viktorov S. V., Shumakher D. A., 1988, *A relationship between the large-scale atmospheric circulation and the origin of coastal upwelling in the Baltic Sea*, Meteorol. Gidrol., 10, 91–98, (in Russian).

Cyberski J., 1997, *Riverine water outflow into the Gulf of Gdańsk*, Oceanol. Stud., 26 (4), 65–75.

Fennel W., Sturm M., 1992, *Dynamics of the western Baltic*, J. Marine Syst., 3 (1)–(2), 183–205.

Gidhagen L., 1984, *Coastal upwelling in the Baltic Sea*, Proc. 14th Conf. Baltic Oceanogr., Gdynia, Vol. 1, 182–190.

Gidhagen L., 1987, *Coastal upwelling in the Baltic Sea – satellite and in situ measurements of sea-surface temperatures indicating coastal upwelling*, Estuar. Coast. Shelf Sci., 24 (4), 449–462.

Haapala J., 1994, *Upwelling and its influence on nutrient concentration in the coastal area of the Hanko Peninsula, entrance of the Gulf of Finland*, Estuar. Coast. Shelf Sci., 38 (5), 507–521.

Horstmann U., 1983, *Distribution patterns of temperature and water colour in the Baltic Sea as recorded in satellite images. Indicators for phytoplankton growth*, Ber. Inst. Meeresk., 106 (1), 147 pp.

Horstmann U., 1986, *Remote sensing of sea surface temperature and water colour anomalies in the southern Baltic Sea*, Bull. Sea Fish. Inst., 17 (5)–(6), 11–17.

ICES (International Council for the Exploration of the Sea) 1969–1980, *Baltic Sea, temperature and salinity*, Oceanographic Data Centre, Copenhagen.

Jankowski A., 2002, *Variability of coastal water hydrodynamics in the southern Baltic – hindcast modelling of an upwelling event along the Polish coast*, Oceanologia, 44 (4), 395–418.

Jędrasik J., 1997, *A model matter exchange and flow of energy in the Gulf of Gdańsk ecosystem – overview*, Oceanol. Stud., 26 (4), 3–20.

Kowalewski M., 1997, *A three-dimensional, hydrodynamic model of the Gulf of Gdańsk*, Oceanol. Stud., 26 (4), 77–98.

Kowalewski M., 1998, *Coastal upwellings in a shallow stratified sea on the example of the Baltic Sea*, Ph. D. thesis, Institute of Oceanography, Univ. Gd., Gdynia, 83 pp., (in Polish).

Krężel A., 1997a, *A model of solar energy input to the sea surface*, Oceanol. Stud., 26 (4), 21–34.

Krężel A., 1997b, *Recognition of mesoscale hydrophysical anomalies in a shallow sea using broadband satellite remote sensing methods*, Diss. and monogr., Univ. Gd., Gdynia, 173 pp., (in Polish).

Lass H.-U., Schmidt T., Seifert T., 1994, *On the dynamics of upwelling observed at the Darss Sill*, Proc. 19th Conf. Baltic Oceanogr., Gdańsk, 247–260.

Lenz W., 1971, *Monatskarten der Temperaturen der Ostsee, dargestellt für verschiedene Tiefenhorizonte*, Dt. Hydrogr. Z., 11, 148 pp.

Lehmann A., Krauss W., Hinrichsen H.-H., 2002, *Effects of remote and local atmospheric forcing on circulation and upwelling in the Baltic Sea*, Tellus, 54 (A), 299–316.

Myrberg K., Andreyev O., 2003, *Main upwelling regions in the Baltic Sea – a statistical analysis based on three-dimensional modeling*, Boreal Environ. Res., 8 (2), 97–112.

Schaffer G., 1979, *Conservation calculations in natural coordinates (with an example from the Baltic)*, J. Phys. Oceanogr., 9 (4), 847–855.

Svansson A., 1975, *Interaction between the coastal zone and the open sea*, Merentutkimuslait. Julk./Havsforskningsinst. Skr., 24, 385–404.

Urbański J., 1995, *Upwellings of the Polish Baltic coast of the Baltic Sea*, Prz. Geofiz., 40 (2), 141–153, (in Polish).

Walin G., 1972a, *On the hydrographic response to transient meteorological disturbances in the Baltic*, Tellus, 24, 169–186.

Walin G., 1972b, *Some observations of temperature fluctuations in the coastal region of the Baltic*, Tellus, 24, 187–198.

Zakharchenko E. N., Kostyukov J. L., 1987, *Forecasts of upwelling in the western Gulf of Riga*, Meteorol. Gidrol., 6, 88–89, (in Russian).